MAASA: Multi-Arm Archimedes Spiral Array for Arrival Angle Estimation

Yuxin Bai[1], Kaikai Li[2] and Xue Li[1, *]

[1] *The 18th Institute of China Academy of Launch Vehicle Technology, Beijing 100023, China*
[2] *Tianjin Key laboratory of Wireless Mobile Communications and Power Transmission, Tianjin Normal University, Tianjin 300387, China*
[*] *Corresponding author e-mail: 13488889707@163.com*

ABSTRACT. *The Direction of arrival (DOA) estimation algorithms to Archimedes spiral antenna remains an important research topic. Unlike the MUSIC algorithm, ESPRIT algorithm has a lower computational complexity. However, ESPRIT algorithm also requires translation invariance, so it can only be used when the array is a uniform planar array (UPA) or a uniform linear array (ULA). This paper introduces a multi-arm Archimedean spiral array (MAASA) ESPRIT algorithm, which transforms the spiral array into a uniform rectangular array through conformal transformation to generate translation invariance. The ESPRIT algorithm is then applied in the transformed domain, and the result is inversely transformed to the initial domain. The simulation results show that the two-dimensional DOA can be realized by using the multi-arm Archimedes spiral array. By comparing the antenna pattern, it is further proved that the multi-arm Archimedes spiral array is superior to the conventional circular array and the planar array.*

KEYWORDS: *Multi-Input Multi-Output, Spiral Array, Archimedes, Angle of Arrival*

1. Introduction

In recent years, increased attention has turned to two-dimensional estimation [1-2] and their practical applications. High performance signal parameter estimation technology in recent years has become very important in radar, sonar, mobile communication and other fields. Since the 1980s, many high performance two-dimensional high-resolution direction-finding methods have been proposed. Among them, MUSIC [3] algorithm and ESPRIT [4-5] algorithm are representative, but ESPRIT algorithm usually requires a special array manifold, which limits its application.

At present, the research and analysis of spatial spectrum estimation of traditional arrays have been carried out in depth. There are few researches on spiral array. Hua

ISSN 2616-5775 Vol. 3, Issue 2: 54-67, DOI: 10.25236/AJCIS.030208

Gudang [6] has studied the DOA estimation of logarithmic spiral arrays. The results show that the logarithmic spiral arrays have higher spatial resolution. The UCA-ESPRIT algorithm proposed in [7] is a breakthrough in the field of circular array two-dimensional DOA estimation. It absorbs the idea of ESPRIT algorithm and realizes two-dimensional DOA estimation. The parameters can be paired automatically. This is a practical array structure, which has applications for radar, satellite communication, sonar, navigation, and smart antenna.

The MUSIC algorithm of Archimedes spiral array has been proposed in [8] and it has shown that Archimedes spiral array improves on traditional circular array and uniform planar array. The ESPRIT algorithm of Archimedes spiral array is studied in this paper based on work done in [8]. The multi-arm Archimedes spiral array is formed by setting the spiral parameters reasonably. The simulation results show that the multi-arm Archimedes spiral array is effective for spatial spectrum estimation and can be extended to MIMO systems.

2. Data Model

In order to simplify the content of the study, this study is based on the following assumptions.

- The source is far-field narrow-band and the signal received by array element is plane wave.
- The weight amplitude of the array element satisfies the uniform distribution, all of which are 1.
- The transmission medium is linear and lossless. The Doppler effect of channel transmission is negligible.
- The signal and noise are independent, and the signal sources are also independent.

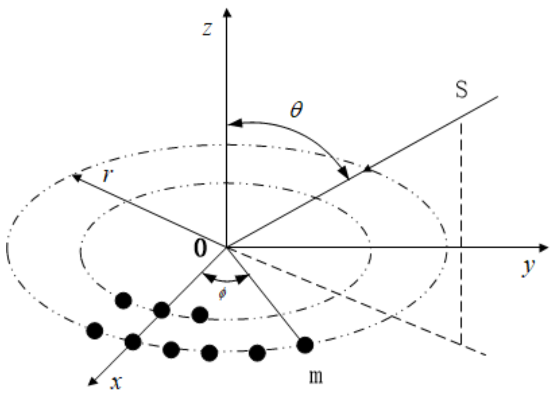

Figure. 1 Data Model

ISSN 2616-5775 Vol. 3, Issue 2: 54-67, DOI: 10.25236/AJCIS.030208

Where the origin of the coordinate system is taken at the center of the circle 0. S indicates that the narrowband signal source radiates from the far field to the array. $\theta \in [0, \pi/2]$ represents the elevation angle of the signal, the angle between the incident direction of the signal and the z-axis. $\phi \in [0, 2\pi]$ is the azimuth angle of the signal, which is the angle projected on the array plane from the x axis along the counter-clockwise direction to the direction of the signal incident.

3. Composition of Multi-arm Archimedes Spiral Array

Archimedes spiral array is an antenna array which arranges elements along Archimedes solenoid according to certain rules. Although Archimedes spiral array is subordinate to a two-dimensional plane array in the rectangular coordinate system, it can be regarded as a linear array in polar coordinates, which is a special array between one and two-dimensional. Therefore, it has also been extensively studied in recent years [9-10]. Archimedes helix polar coordinates are expressed as follows.

$$r = a + b \cdot \phi \tag{1}$$

Where r is the distance from the point on the helix to the origin of the coordinate, and a is the distance from the starting point to the origin of the polar coordinate. b is the angular velocity of spiral rotation, controlling the distance b etween two adjacent curves. The plane Cartesian coordinate equation of Ar chimedes helix is as follows.

$$x = r \cdot \cos(\phi) \tag{2}$$

$$y = r \cdot \sin(\phi)$$

The structure of the unevenly placed single-arm Archimedes spiral array is shown in Figure 2, with the following parameters.

$$\phi \in [\frac{\pi}{2}, 4\pi] \tag{3}$$

a=0.2, b=0.2

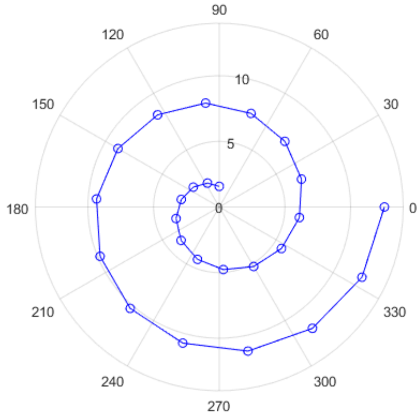

Figure. 2 Structure of single-arm Archimedes Spiral Array with non-uniformly placed Array elements

According to the antenna theory, the random distribution of the array elements can eliminate the sidelobe, enlarge the aperture of the array element, eliminate the false spectral peak, and make the array achieve the purpose of high resolution. Planar arrays have ring arrays, rectangular arrays, L-shaped arrays and so on, but they are uniform arrays. The Archimedes spiral array is more than half the wavelength of the Archimedes spiral due to the small number of elements, and the pseudo-random object of the array element is achieved, so that the periodicity of the occurrence of the grating lobe is suppressed, and the distance between the array elements is increased, and the coupling is reduced.

With parameter $\phi \in [0, \frac{\pi}{4}]$, a=0.1,b=0.2, a single-armed Archimedes spiral is obtained, which is rotated counterclockwise, in turn, resulting in a total of 8 spirals. The multi-arm Archimedes spiral array plane model is shown in Figure 3. There are 8 array elements on each spiral line, the total number of array elements is 64, and the array elements on the same spiral line are rotated counterclockwise by $\frac{\pi}{32}$. By setting the spiral parameters reasonably, the multi-arm Archimedes spiral array is formed. As parameter values of a, b, ϕ are determined, the array structure is also determined.

ISSN 2616-5775 Vol. 3, Issue 2: 54-67, DOI: 10.25236/AJCIS.030208

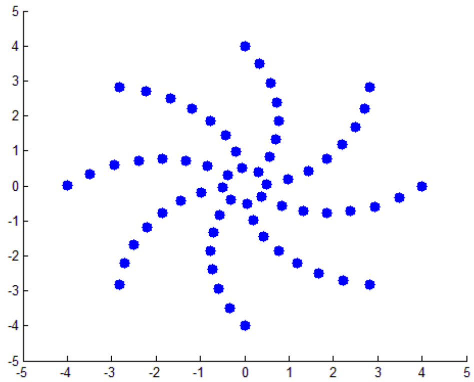

Figure. 3 Schematic diagram of multi-arm Archimedes spiral array

4. Conformal Transformation

Geometry is composed of points. If a mapping transforms one point in the original geometry into another point in the new graph, the original geometry can be transformed into another geometric figure. An original irregular figure can often be transformed into a regular graph after choosing the appropriate mapping. Subsequently, the regular graph is easy to solve because of its simplicity, and the obtained solution can then be converted back to the original graph. The solution of the original graph problem can be obtained, and the conformal transformation is such a mapping.

Let G be a nonempty set of complex number $z = x + iy$, existence rule f, such that $\forall z \in G$, there is a corresponding $w = u + iv$, then the complex function w is a function of the complex variable z. As Formula (4) shows.

$$\begin{cases} u = u(x, y) \\ v = v(x, y) \end{cases} \tag{4}$$

In geometry, $w = f(z)$ can be regarded as the mapping of $z \in G$ (z plane) $\rightarrow w \in G'$ (w plane), w is the image point of z, z is the original image of w, and the transformation f is called conformal transformation.

Conformal transformation consists of two basic transformations: amplitude transformation and angle transformation. The function of amplitude transformation is to stretch the length of the line segment, while the function of angle transformation is to change the slope of the line. Angle transformation can be expressed as Formula (5).

$$f(z) = c\angle \arg(z) \tag{5}$$

ISSN 2616-5775 Vol. 3, Issue 2: 54-67, DOI: 10.25236/AJCIS.030208

The effect of the angle transformation is shown in the following illustration, and the angle transformation converts a line with a certain angle to the horizontal axis into a horizontal line as Figure 4 shows.

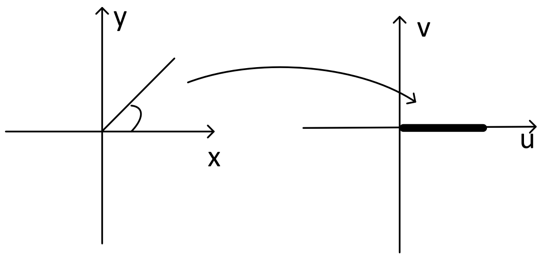

Figure. 4 Angle transformation

Conformal transformation is widely used in electromagnetic field problems. The known complex boundary problem can be transformed into a simple boundary by conformal transformation, and the simple boundary usually has a mature solution. After the solution is successfully solved, the solution of the original problem can be obtained by inversely transforming it into the original problem.

5. Two-dimensional ESPRIT Algorithm for Multi-arm Archimedes Spiral Array

The ESPRIT algorithm depends on the translation invariance of the array, but the Archimedes spiral array is not directly translational invariant, but the array is transformed into a uniform rectangular array after conformal transformation. Therefore, the actual direction of the wave can be obtained by the ESPRIT algorithm. The 8-arm Archimedes spiral array does not directly have translational invariance. However, based on the form of the array and the $\frac{\pi}{4}$ rotation of the 8-arm, it can be seen that the array can be transformed into a uniform rectangular array after conformal transformation to generate translational invariance. Thus, the angle of arrival in the transform domain can be obtained by the ESPRIT algorithm, and the direction of the actual wave can then be obtained by inverse transformation, which is corroborated by the simulation results.

Eight segments parallel to the x axis can be obtained by conformal transformation of the eight spiral arms, which are showed in Formula (6).

$$\begin{aligned} &y=0,\quad y=d,\quad y=2d,\quad y=3d \\ &y=4d, y=5d, y=6d,\quad y=7d \end{aligned} \tag{6}$$

Because there are eight elements on each arm and eight elements can be obtained by conformal transformation, a uniform rectangular array of 8×8 is formed, as shown in Fig. 5.

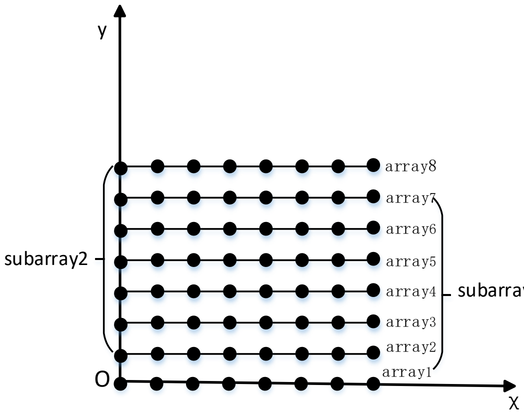

Figure. 5 Transformation diagram

Therefore, we can estimate the two-dimensional angle of ESPRIT based on the uniform spacing rectangular antenna array shown in Figure 5, which is the generalization of one-dimensional ESPRIT algorithm. The formula of two-dimensional ESPRIT algorithm is derived below. The direction matrix of the eight elements located on the x -axis is B_x , and the coordinate of the Archimedes Spiral element before transformation is $p=(r_i\cos\phi_i, r_i\sin\phi_i)$, the coordinates of the elements on the transformed rectangular array are $p=(\phi_i, d)$. However, the pitch angle θ in the direction of the incoming wave is the Angle included with the Z-axis, while the Z-axis does not change. Therefore, $\theta=\theta^{'}$ remains unchanged before and after the transformation. The transformation $f(r)=\left|r\right|-\frac{d}{\phi_0}\angle\arg(r)$, where $-\frac{d}{\phi_0}\angle\arg(r)$ is an angle transformation. As a result, the azimuth is $\phi^{'}=\phi-\frac{d}{\phi_0}\phi$, where ϕ is the azimuth before transformation, and $(\theta^{'},\phi^{'})$ is the angle of arrival in the transform domain.

Let the array element number of a plane array be $M\times N$, the number of sources is K. θ_k and ϕ_k represent the elevation and azimuth of the kth source, respectively.

ISSN 2616-5775 Vol. 3, Issue 2: 54-67, DOI: 10.25236/AJCIS.030208

Then the wave path difference between the space ith element and the reference element is shown in Formula (7).

$$\beta_{ij}(\theta,\phi)=2\pi(x_i\cos\phi\sin\theta+y_j\sin\phi\sin\theta)/\lambda \tag{7}$$

Where, $x_i=\phi_i, y_j=(j-1)d$, (x_i, y_i) are the coordinates of the ith element, and the plane array is generally in the $x-y$ plane, the general z_i is 0.

The directional matrix of the 8 elements on the x axis is B_X, the directional matrix of 8 elements on the y axis is B_Y, So the directional matrix B_X corresponding to the 8 elements on the x axis is defined as Formula (8).

$$B_x=\begin{bmatrix} e^{-j\omega\beta_{11}(\theta_1,\phi_1)} & e^{-j\omega\beta_{11}(\theta_2,\phi_2)} & \cdots & e^{-j\omega\beta_{11}(\theta_D,\phi_D)} \\ e^{-j\omega\beta_{21}(\theta_1,\phi_1)} & e^{-j\omega\beta_{21}(\theta_2,\phi_2)} & \cdots & e^{-j\omega\beta_{21}(\theta_D,\phi_D)} \\ \vdots & \vdots & \ddots & \vdots \\ e^{-j\omega\beta_{81}(\theta_1,\phi_1)} & e^{-j\omega\beta_{81}(\theta_2,\phi_2)} & \cdots & e^{-j\omega\beta_{81}(\theta_D,\phi_D)} \end{bmatrix} \tag{8}$$

In the same way, we can get the direction matrix B_Y corresponding to 8 elements on the y axis. Because the directional matrices of other arrays parallel to the x axis have to consider the deviation along the y axis, the wave path difference of each element relative to the reference element is equal to the wave path difference of the element of array 1 plus $2\pi d\sin\phi\sin\theta/\lambda$, so we can obtain submatrix m in Formula (9).

$$B_m=B_xD_m(B_y) \quad (m=1,2,\cdots,8) \tag{9}$$

Where, $D_m(\cdot)$ is a diagonal matrix constructed from m rows of a matrix. Thus, the received signal of the rectangular array can be expressed as follows.

$$x(t)=\begin{bmatrix} B_xD_1(B_y) \\ B_xD_2(B_y) \\ \vdots \\ B_xD_8(B_y) \end{bmatrix} s(t)+n(t) \tag{10}$$

The translational invariance of the rectangular array allows it to be decomposed into two subarrays. Each subarray contains 7 linear arrays, and the subarray 1 is an antenna array composed of the following 7 parallel arrays. The subarray 2 is an antenna array composed of 7 parallel arrays above, and the subarray 2 can be transformed into a subarray 1 by the downward translation of d.

ISSN 2616-5775 Vol. 3, Issue 2: 54-67, DOI: 10.25236/AJCIS.030208

The rotation invariance of the direction matrix can be obtained from the translation invariance of the rectangular array. Let the direction matrix of the subarray 1 be A_1 and the direction matrix of the subarray 2 be A_2, and the rotation relation can be obtained as follows.

$$A_2 = A_1\Phi \tag{11}$$

where $\Phi = \mathrm{diag}(\sin\theta_1 e^{j\phi_1} \quad \sin\theta_2 e^{j\phi_2} \quad \cdots \quad \sin\theta_2 e^{j\phi_2})$ is called the rotation operator, which relates the output of the submatrix $x_1(k)$ and $x_2(k)$.

The received signals of the two arrays together are notated as $x(k)$.

$$\begin{aligned} x(k) &= \begin{bmatrix} x_1(k) \\ x_2(k) \end{bmatrix} = \begin{bmatrix} A_1 \\ A_1\cdot\Phi \end{bmatrix}\cdot s(k) + \begin{bmatrix} n_1(k) \\ n_2(k) \end{bmatrix} \\ &= As(k) + n(k) \end{aligned} \tag{12}$$

Two signal subspaces E_1 and E_2 can be obtained by decomposing the covariance matrix of two subarrays. Because the antenna array has a parallel shift relationship, the signal subspace has a rotation relationship, which can be expressed as follows.

$$E_1\psi = E_2 \tag{13}$$

In addition, the signal subspace with known properties is the same as the steering vector space, so there exists a unique nonsingular $D \times D$ full rank matrix T .

$$\begin{aligned} E_1 &= A_1 T \\ E_2 &= A_1\phi T \end{aligned} \tag{14}$$

From (12) and (13),

$$T\Psi T^{-1} = \Phi \tag{15}$$

Formula(15) is the decomposition of the eigenvalue of ψ . According to the TLS criterion [15], the eigenvalue of ψ can be estimated and decomposed. The eigenvalue obtained is the function of the azimuth and elevation angle. The corresponding eigenvalue is $\mu_i\,(i = 1,\cdots,P)$, which is further calculated as follows.

$$\hat{\theta}_i = \arcsin(|\mu_i|), \hat{\phi}_i = angle(\mu_i) \tag{16}$$

ISSN 2616-5775 Vol. 3, Issue 2: 54-67, DOI: 10.25236/AJCIS.030208

6. Simulation and Performance Analysis

In order to evaluate the performance of multi-arm Archimedes spiral array in DOA estimation, we do the following simulation and pattern comparison.

Simulation 1: The signal source is the zero mean Gao Si source P=2, the number of array elements M=64, the number of snapshots N=512, the SNR is 0dB and 10dB, respectively. The azimuth can be get by follows.

$$\phi = [30,40] \cdot \frac{\pi}{180} \tag{17}$$

The elevation angle is,

$$\theta = [15,30] \cdot \frac{\pi}{180} \tag{18}$$

Use ESPRIT algorithm after conformal transformation of Archimedes spiral array. We did 100 Monte Carlo simulation experiments. The SNR of Figure 7 is 0dB, and Figure 6 is 10dB. The simulation results are as shown in the figure.

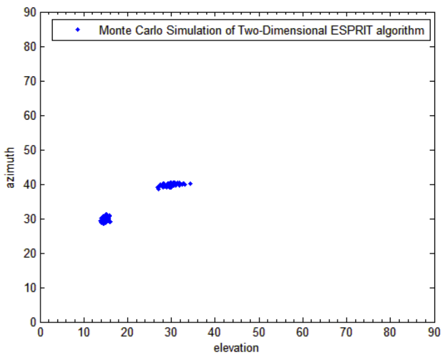

Figure. 6 SNR=0dB

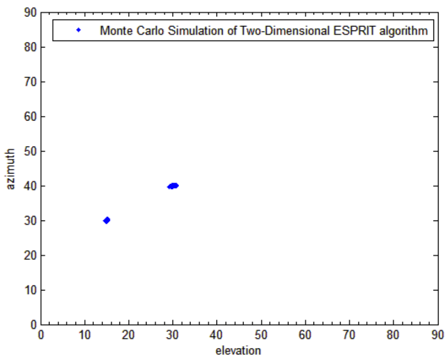

Figure. 7 SNR=10dB

Simulation 2: The signal source is an AM signal; the modulation frequency is 1.5KHz, 4.0KHz, respectively. The number of array elements M=64. Snapshots is 256.SNR=0dB. The azimuth $\phi = [20,40] \cdot \frac{\pi}{180}$ and the elevation angle $\theta = [15,30] \cdot \frac{\pi}{180}$. Use ESPRIT algorithm after conformal transformation of Archimedes spiral array. We performed 100 Monte Carlo simulation experiments, which are shown in figure 8.

ISSN 2616-5775 Vol. 3, Issue 2: 54-67, DOI: 10.25236/AJCIS.030208

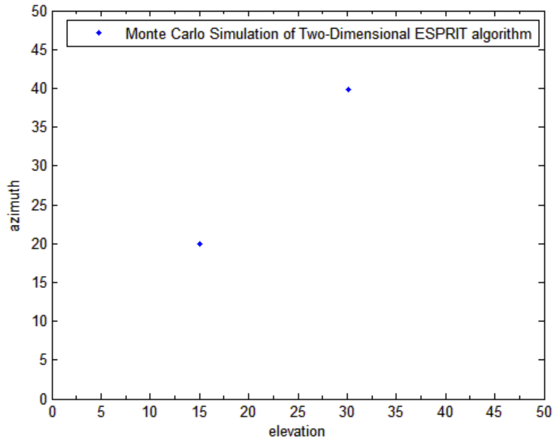

Figure. 8 AM signal simulation diagram

Through the simulation, it can be seen that the ESPRIT algorithm of multi-arm Archimedes spiral array can estimate the arrival angle of the signal, improve the signal-to-noise ratio, and adopt the AM signal. The simulation result is improved, and the simulation diagram is more accurate.

Let's consider M array antenna elements, and take the coordinate origin O as the reference point, the position of the m array element in the array is (x_m, y_m, z_m), its field intensity radiation pattern is $f_m(\phi,\theta)$, and the phase and amplitude weighting coefficients of each antenna element are α_m and A_m, respectively. A constant term that removes the common phase factor and amplitude. Then the pattern of all antenna elements in the (ϕ,θ) direction of the entire array can be expressed as follows.

$$F(\phi,\theta)=\sum_{m=1}^{M} f_m(\phi,\theta)A_m e^{j(\frac{2\pi}{\lambda}\Delta R_m-\alpha_m)} \tag{19}$$

In the formula above, ΔR_m is the difference between the distance from the m antenna element to the target and the distance from the reference point O to the target, and λ is the wavelength of the received signal.

The antenna pattern of 64-element multi-arm Archimedes spiral array is shown in Figure 9. The antenna beam width is $\theta_{3dB}=8^{\circ}$ and the proximal sidelobe level is $SLL=-9\mathrm{d}B$.

ISSN 2616-5775 Vol. 3, Issue 2: 54-67, DOI: 10.25236/AJCIS.030208

For comparison, a 8×8 uniform planar array (UPA) with a cell pitch of half wavelength is taken, and the antenna pattern of the antenna is shown in Figure 10, the antenna beam width is $\theta_{3dB} = 23^{\circ}$, and the proximal sidelobe level is $SLL = -12\text{d}B$. Compared with 64 circular arrays, the excitation amplitude is 1 and the excitation phase is 0. The radiation pattern is shown in Figure 11. The antenna beam width is $\theta_{3dB} = 15^{\circ}$ and the proximal sidelobe level $SLL = -7\text{d}B$. It can be seen from the comparison that the beam width of conventional UPA is obviously higher than that of UCA, MAASA. When the apertures of UCA and MASA antenna are about the same size, the sidelobe level of UCA antenna is slightly higher than that of MAASA antenna, and the beam-width of UCA antenna is not as sharp as MAASA antenna.

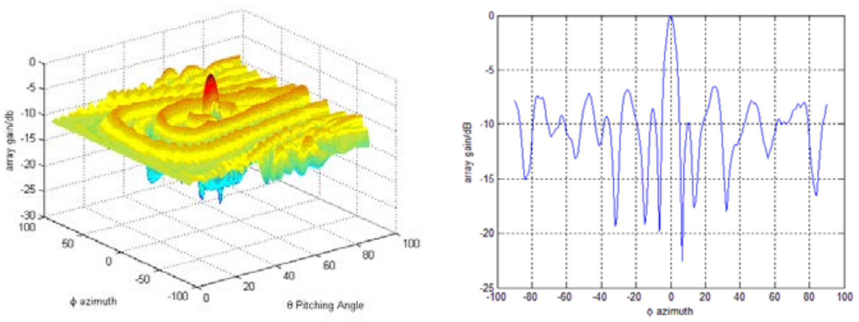

Figure. 9 Pattern of multi-arm Archimedes spiral array antenna

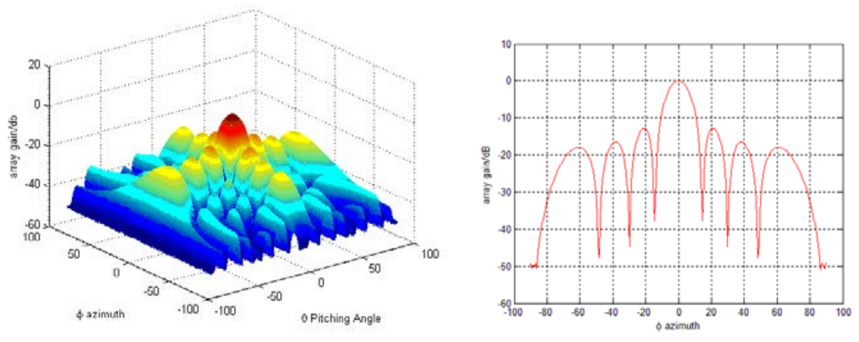

Figure. 10 8×8 *Planar Array Antenna pattern*

ISSN 2616-5775 Vol. 3, Issue 2: 54-67, DOI: 10.25236/AJCIS.030208

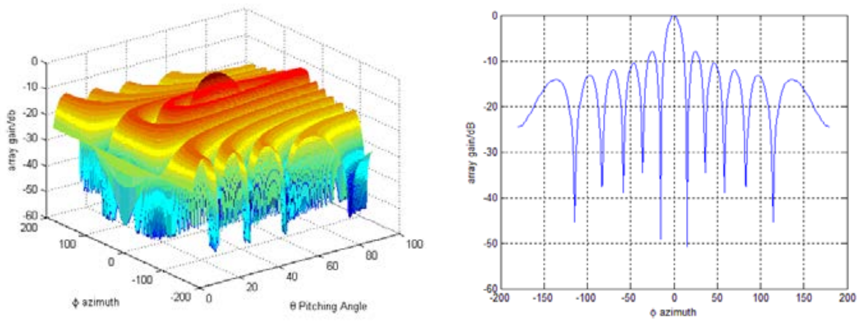

Figure. 11 Uniform circular array antenna pattern

7. Conclusion

This paper proposes a multi-arm Archimedes spiral array (MAASA) that improves upon existing methods. In this paper, we study the non-coherent sources only. Simulation results are verified by ESPRIT algorithm, and the spatial spectrum estimation is realized. Compared with different antenna patterns, the performance of multi-arm Archimedes spiral array provides better results than UCA or other traditional array does.

References

[1] C. P. Mathews, M. D. Zoltowski, "Eigenstructure Techniques for 2-D Angle Estimation with Uniform Circular Array", IEEE Transactions on Signal Processing, vol. 42, no. 9, pp. 2395-2407, 1994.

[2] P. Strobach, "Total Least Squares Phased Averaging and 3-D ESPRIT for Joint Azimuth-Elevation-Carrier Estimation", IEEE Transactions on Signal Processing, vol. 49, no. 1, pp. 54-62, 2001.

[3] M. Wax, T. Shan, T. Kailath, "Spatio-temporal spectral analysis by eigenstructure method", IEEE Transactions on Acoustic, Speech, and Signal Processing, vol. 32, no. 4, pp. 817-827, 1984.

[4] R. Roy, T. Kailath, "ESPRIT-estimation of Signal Parameters Via Rotational Invariance Techniques", IEEE Transactions on Acoustic, Speech, and Signal Processing, vol. 37, no. 7, pp. 984-995, 1989.

[5] A. Paulraj, R. Roy, T. Kailath, "A subspace rotation approach to signal parameter estimation", Proceedings of the IEEE, vol. 74, no. 7, pp. 1044-1046, 1986.

[6] G. Hua, Y. Dong, W. Hong, "Direction of arrival estimation based on logarithmic helical array", Journal of Radio Science, vol. 24, no. 12, pp. 987-991, 1008, 2009.

ISSN 2616-5775 Vol. 3, Issue 2: 54-67, DOI: 10.25236/AJCIS.030208

[7] C. P. Mathews, M. D. Zoltowski, “Eigenstructure techniques for 2-D angle estimation with uniform circular array”, IEEE Transactions on Signal Processing, vol. 42, no. 9, pp. 2395-2407, 1994.
[8] J.Chen, S. Guan. Y, Tong, L. Yan, “Two-Dimensional Direction of Arrival Estimation for Improved Archimedean Spiral Array With MUSIC Algorithm”, IEEE Access, vol. 6, pp. 49740-49745, 2018.
[9] K. P. Morrison, G. W. Keilman, P. J. Kaczkowski, “Single archimedean spiral close packed phased array HIFU”, Proceedings of the IEEE International Ultrasonics Symposium, pp. 400-404, Chicago, IL, USA, 2014.
[10] J. J. V. Tonder, J. K. Cloete, “A study of an Archimedes spiral antenna”, Proceedings of the Antennas and Propagation Society International Symposium, pp. 1302-1305, Seattle, WA, USA, 1994.